Crossref

IJBSM March 2026, 17(3): 01-12

Article AR6704

Research Article

Natural Resource Management

DOI: HTTPS://DOI.ORG/10.23910/1.2026.6704

Estimation of Surface Runoff for Mahatma Phule Krishi Vidyapeeth Central Campus, Ahilyanagar, Maharashtra, Using Remote Sensing and Geographical Information System

S. B. Nandgude, H. S. Ganachari, S. S. Shinde, D. D. More, M. D. Chavan, B. S. Kamble, V. V. Patil and O. N. Khapke

Dept. of Soil and Water Conservation Engineering, Dr. A.S.C.A.E. and T., M.P.K.V., Rahuri, Ahilyanagar, Maharashtra (413 722), India

Open Access

Corresponding 01swce14@gmail.com

0000-0002-6157-9242

ABSTRACT

The experiment was conducted during the month of December to May, 2024 at the department of Soil and Water Conservation Engineering, Dr. Annasaheb Shinde College of Agricultural Engineering and Technology, Rahuri, Maharashra, India for watershed planning and Management study at Mahatma Phule Krishi Vidyapeeth Central Campus, Ahilyanagar, Maharashtra. This study estimated annual run-off in 2021 for a 475 ha micro-watershed within the Mahatma Phule Krishi Vidyapeeth (MPKV) Central Campus (West), situated between 19°19' to 19°22' N latitude and 74°36' to 74°40' E longitude, using the Soil Conservation Service – Curve Number (SCS-CN) method integrated with ArcGIS 10.5. Essential thematic layers, including stream order, digital elevation model (DEM), hydrologic soil group (HSG), curve number (CN), and land use/land cover (LULC) maps, were generated to support spatial analysis and runoff computation. The weighted curve numbers determined for antecedent moisture conditions I, II, and III were 53.53, 73.28, and 86.32, respectively. Results showed that the watershed experienced an annual surface runoff depth of 278.97 mm, corresponding to 28.86% of the 966.40 mm total rainfall during 2021. The derived runoff estimates provide a critical baseline for designing water-harvesting and soil-conservation structures. Furthermore, these pre-development runoff values serve as a reference for evaluating the effectiveness and impact of future soil and water conservation interventions within the watershed.

KEYWORDS: Remote sensing, GIS, curve number

***Citation* (VANCOUVER):** Nandgude et al., Estimation of Surface Runoff for Mahatma Phule Krishi Vidyapeeth Central Campus, Ahilyanagar, Maharashtra, Using Remote Sensing and Geographical Information System. *International Journal of Bio-resource and Stress Management,* 2026; 17(3), 01-12. HTTPS://DOI.ORG/10.23910/1.2026.6704.

Data Availability Statement: Legal restrictions are imposed on the public sharing of raw data. However, authors have full right to transfer or share the data in raw form upon request subject to either meeting the conditions of the original consents and the original research study. Further, access of data needs to meet whether the user complies with the ethical and legal obligations as data controllers to allow for secondary use of the data outside of the original study.

Conflict of interests: The authors have declared that no conflict of interest exists.

RECEIVED on 19th September 2025 RECEIVED in revised form on 05th February 2026 ACCEPTED in final form on 19th February 2026 PUBLISHED on 27th February 2026

1. INTRODUCTION

Surface runoff, the excess precipitation exiting a catchment after filling surface and subsurface storage, results from the interaction of storm properties (e.g., intensity, duration) with basin characteristics such as soil type, hydrologic group, slope, land use, vegetation, and antecedent moisture conditions (Sun et al., 2021; Fan et al., 2019). Accurate estimation of runoff typically depends on factors such as precipitation, basin recharge dynamics, and catchment characteristics. However, in India, the availability of continuous runoff datasets remains notably limited, necessitating the development and adoption of reliable indirect estimation techniques (Al-Ghobari et al., 2020). Foremost among these is the Soil Conservation Service Curve Number (SCS-CN) method, which relates storm rainfall to direct runoff through a single, physically interpretable parameter that aggregates land use, soil type, and hydrologic conditions (Jakir Hussain et al., 2024; Soulis et al., 2009; Govindaraju, 2024), and is widely applicable across diverse agro-climatic regions (Pandey et al., 2021). The method is especially widely used in India, both for research and for practical watershed management (Gupta et al., 2015; Singh et al., 2023). Because of its modest data requirements, transparent formulation, and ease of embedding within spatial platforms, SCS-CN has become a mainstay for hydrologic design and planning at event to annual scales. Its applications range from large-scale river basin hydrological modeling (Soulis, 2021) to the prioritization of micro-watersheds for conservation structures (Halder et al., 2024). Accurate runoff prediction is essential for planning water harvesting structures and reducing sedimentation and downstream flooding risks (Chimdessa et al., 2023). The integration of remote sensing (RS) and geographic information system (GIS) technologies has significantly improved spatially explicit watershed assessment and runoff modeling (Reddy et al., 2020). GIS enables efficient analysis of spatial data such as DEM, soil, and land cover for SCS-CN computations (Srivastava, 2016). Studies confirm the effectiveness of RS-GIS-based runoff modeling for prioritizing water harvesting and resource management (Meshram and Sharma et al., 2017; Muneer et al., 2020). Some literature demonstrates that such GIS-enabled implementations of SCS-CN are both tractable in semi-arid and sub-humid agricultural landscapes, where localized interventions for soil and water conservation, groundwater recharge, and flood moderation are urgently needed (Chavda et al., 2016; Sishah, 2021; Shiv et al., 2023; Nikita et al., 2024; Raushan et al., 2024; Jha et al., 2014). Recent studies offer key insights: (i) runoff percentages are highly sensitive to LULC composition and hydrologic soil group assignments (Gupta and Dixit, 2022; Kadam et al., 2019); (ii) slope and drainage density influence infiltration time and runoff generation (Deshmukh et al., 2013); and (iii) antecedent moisture condition (AMC) strongly affects predicted runoff, especially during short, intense storms (Grillakis et al., 2016). Empirically, agricultural watersheds show moderate runoff (≈20–35%) (Bansode and Patil, 2014; Garg et al., 2013), while forested basins yield lower values (≈5–15%) (Satheeshkumar et al., 2017; Kumar et al., 2021). This study applies an integrated RS/GIS–SCS-CN method to the 475-ha MPKV Central Campus (West) watershed using ArcGIS 10.5 for runoff estimation in 2021. The approach supports LULC scenario modeling, micro-watershed prioritization, and flood risk assessment. Machine-learning models may outperform SCS-CN in data-rich basins (Gabriels et al., 2021; Garzón et al., 2022). Classical critiques of the SCS-CN method—particularly regarding the initial abstraction ratio, soil moisture handling, and AMC classifications—highlight the need for recalibration to reduce systematic bias (Mishra and Singh, 2003; Soulis, 2021). Indian studies further stress the importance of validating SCS-CN outputs with observed hydrographs or proxy indicators like reservoir inflows and groundwater responses to enhance reliability (Katpatal et al., 2014; Singh et al., 2023; Wang et al., 2025). The study aimed to balance rapid runoff estimation with actionable planning for water harvesting, recharge augmentation, and downstream hazard mitigation.

2. MATERIALS AND METHODS

2.1. Study area

The present study area is the Mahatma Phule Krishi Vidyapeeth Central Campus (West) Watershed, located in Rahuri taluka of Ahmednagar district, Maharashtra (Figure 1). Ahmednagar district is the largest district of Maharashtra state in western India. The area is located between 19°19' to 19°22' North latitude and 74°36' to 74°40' East longitude. The total area of the watershed is

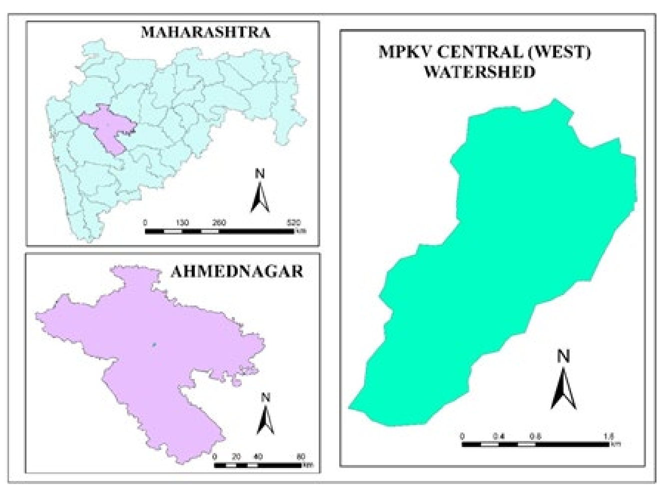

Figure 1: Location of the study area

475 ha. The MPKV Central Campus watershed is situated under the basin of the Mula River. Climatically, the area falls under the tropical zone with an average annual rainfall of 511 mm. The average annual temperature is 25.9°C. The annual mean maximum and minimum relative humidity range from 59 to 90 and 21 to 61%, respectively.

2.2. Data collection and software used

As per the requirements of the study, a variety of data were collected from various sources, as detailed below:

1. Digital Elevation Model (DEM) (http://bhuvan-noeda.nrsc.gov.in)

2. Digital Imagery Data: Sentinel 2 MSI L1C (http://scihub.copernicus.eu)

3. Soil data

4. Rainfall data, mm

Rainfall data for the year 2021 were collected from the IMD observatory located at AICRP on Irrigation Water Management, MPKV, Rahuri, shown in Figure 2.

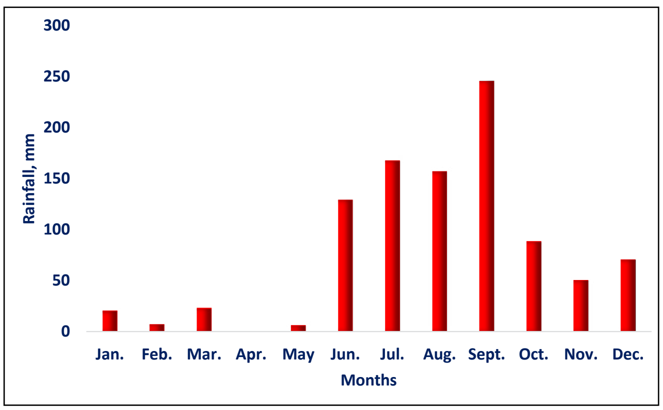

Figure 2: Monthly rainfall data (mm) for the year 2021

2.3. Software and system

Arcs-GIS 10.5 and MS-Office suite were used for data creation, data analysis, and output generation. Arcs-GIS 10.5 is an advanced tool used for mapping, geographic analysis, spatial analysis, hydrology, overlay analysis, data editing, etc. MS-Office was used for documentation analysis purposes.

2.4. Delineation of watershed

Arcs-GIS 10.5 was used for watershed delineation using the Survey of India toposheet (1:50,000 scale). Toposheets provide information related to the location, drainage network, and contours. 47 I/11 numbered toposheet was used for watershed delineation. The flow chart of methodology is presented in Figure 3, which shows various steps involved in the utilization of input parameters, like toposheet, satellite data, for getting the final output of the water resources conservation plan.

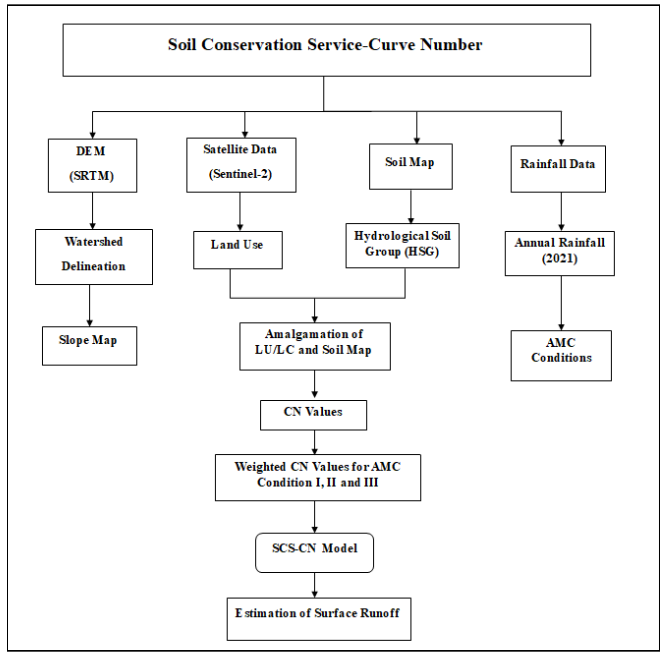

Figure 3: Flow chart for runoff estimation

2.5. Generation of thematic maps

All the thematic maps, viz., base map, stream order, DEM, slope, flow direction, flow accumulation, HSG, CN map, and land use/land cover, were generated in ArcGIS 10.5 software. The stream order map was generated from DEM data. The flow accumulation and flow direction maps were prepared by processing DEM data in ArcGIS software, which is further used to generate a stream network. After generating the stream network, identify the stream order in the watershed. The stream order map is presented in Figure 4.

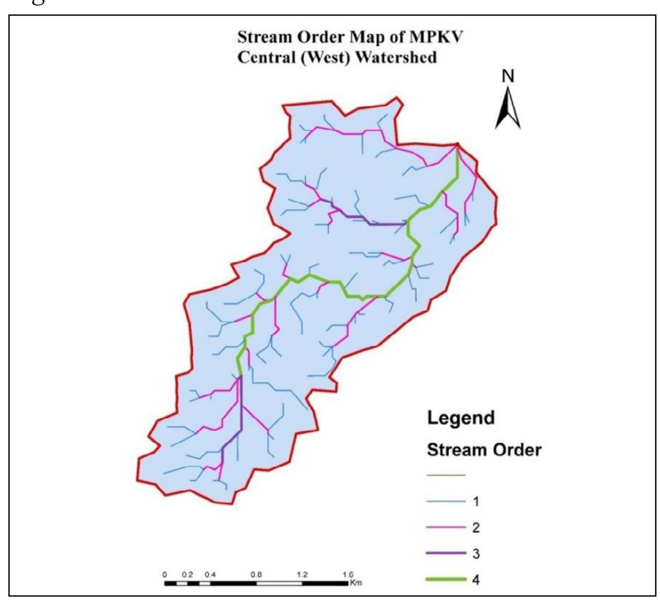

Figure 4: Stream order map of MPKV Central (West) Watershed

2.6. *Land use/land cover*

The identification of land use/land cover is an important aspect for various planning and management activities in the watershed. Land cover refers to vegetation, water bodies, rocks/soil, artificial cover, and others resulting from transformations. A land use/land cover map of the study area was prepared by Supervised Classification using a cloud-free satellite image, Sentinel 2 MSI L1C 2021 was downloaded from (https://scihub.copernicus.eu).

2.7. *Soil mapping and hydrological soil groups*

Hydrological Soil Groups (HSGs), which categorize soils by infiltration and water transmission rates, significantly influence runoff. The SCS-CN (NRCS) method uses HSGs to define hydrological parameters, primarily the infiltration rate of bare, saturated soil. The four HSGs are:

Hydrologic Soil Groups (HSGs) are classified as follows:

Group A: High infiltration rates, even when saturated (e.g., deep, well-drained sands and gravels).

Group B: Moderate infiltration rates when saturated (e.g., moderately deep, well-drained soils with moderate textures).

Group C: Low infiltration rates when saturated (e.g., soils with restrictive layers or fine textures).

Group D: Very low infiltration rates when saturated (e.g., clay soils with high swelling potential, high water tables, or shallow soils over impermeable layers).

The curve number for different hydrological soil groups with antecedent moisture content II was used for the estimation of the weighted curve number, which is given in Table 1.

Table 1: Curve number for HSG under AMC-II conditions (Ahmad et al., 2015)

Classes	Hydrological soil group			
	A	B	C	D
Agriculture land	76	86	90	93
Built up	69	79	84	87
Forest	26	40	58	61
Barren land	71	80	85	88
Waterbodies	97	97	97	97

2.8. *Runoff estimation by SCS-CN (NRCS) method*

The Curve Number (CN) method, originally developed by the U.S. Soil Conservation Service (SCS) (1964, 1972) and now known as the NRCS method, estimates runoff based on a water balance equation for a specified time interval, which is given as.

$P=I_a+F+Q$ 1

Where,

P=Total precipitation, mm

I_a=Initial abstraction, mm

F=Cumulative infiltration, mm

Q=Direct surface runoff, mm

Runoff was estimated using the SCS-CN (NRCS) method, taking into account different combinations of soil groups, land use types, and antecedent moisture conditions (AMC). Daily rainfall data were used with the Curve Number method, which doesn't explicitly account for time. In ungauged basins, this method estimates direct runoff depth from rainfall, using a runoff response index. Its simplicity and flexibility contribute to its widespread use. The method centers on the watershed's potential maximum retention (S), determined by AMC and watershed characteristics. Overall methodology adopted in the study for estimating runoff is depicted in Figure 3.

The retention capacity (S) of the watershed can be predicted in terms of a dimensionless parameter curve number (CN), and given by,

$S=(25400/CN)-254$ 2

Where,

S=Maximum recharge capacity of the watershed after 5 days of antecedent rainfall

CN=Curve number

The direct runoff of the watershed is given by the following equation,

$Q=0$ If $p<=0.2S$ 3

$Q=(P-0.2S)^2/(P+0.8S)$ If $p>=0.2S$.................................... 4

Where,

Q=Runoff depth, mm

P=Rainfall, mm

S=Maximum recharge capacity of the watershed after 5 days of antecedent rainfall.

2.8.1. *Calculation for CN*

A CN map was created in a GIS environment by integrating HSG and land use maps. The weighted curve numbers for each micro-watershed were determined by multiplying the area of each land use class by its respective curve number. A weighted CN map was generated using the following equation,

$CN= (\sum CN_i \times A_i)/A$ 5

Where,

CN=Weighted curve number

CN_i=Curve number from 1,2, 3, i

A_i=Area with curve number CN_i

A=Total area of the watershed

2.8.2. Antecedent moisture condition (AMC)

The CN method uses three antecedent moisture conditions (AMCs): AMC-I (dry), AMC-II (normal), and AMC-III (wet). Table 2 shows the seasonal rainfall limits for each AMC.

Table 2: Group of antecedent soil moisture classes (AMC)

AMC group	Soil characteristics	Five-day antecedent rainfall (mm)	
		Dormant season	Growing season
I	Soil is dry but not to the wilting point. Satisfactory cultivation has taken place (Dry condition)	Less than 13	Less than 36
II	Average condition	13-28	36-53
III	Sufficient rainfall has occurred within the immediate past 5 days. Saturated soil conditions prevail (Wet condition)	Over 28	Over 53

CN for AMC I $CN_I=(4.2\times CN_{II})/(10-(0.058\times CN_{II})$ 6

CN for AMC III $CN_{III}=(23\times CN_{II})/(10+(0.13\times CN_{II})$ 7

To calculate CN values for AMC-1 and AMC-III conditions, the following equations were used (Chow et al., 1988),

Where,

CN I=Curve number for dry condition

CN II=Curve number for normal condition

CN III=Curve number for wet condition

Daily rainfall data from 2021 and the maximum potential retention (S) values derived from the watershed's CN were used to estimate runoff using the SCS-CN (NRCS) model.

3. RESULTS AND DISCUSSION

3.1. Delineation of the watershed

In this study, the boundary of the MPKV Central Campus (West) watershed was delineated by integrating Survey of India topographic sheets at a 1:50,000 scale with a 30 m resolution ASTER Digital Elevation Model (DEM), following georeferencing and rectification within ArcGIS. This methodological choice reflects recent hydrological research that emphasizes the integration of DEMs with authoritative cartographic sources to improve watershed delineation accuracy. For instance, Khalid et al. (2021) compared ASTER and SRTM DEMs in Johor, Malaysia, and found ASTER to be more reliable in capturing drainage networks in complex terrain. Similarly, Shaikh et al. (2022) demonstrated that ASTER and CARTOSAT DEMs yield comparable watershed boundaries in Gujarat, with ArcSWAT-based delineation achieving minimal error margins. Nasrin and Barman (2023) further highlighted the utility of ASTER DEM in digital terrain analysis for the Jamuna watershed of Assam, showing that slope, aspect, and stream order maps derived from ASTER data provide robust morphometric characterization in data-scarce regions. More recently, Memon et al. (2025) statistically evaluated multiple open-source DEMs-including ASTER, CARTOSAT, and SRTM-and confirmed that ASTER remains a robust option for sustainable river basin management when validated against field data. Collectively, these studies reinforce the approach adopted here: integrating DEMs with topographic maps reduces boundary misclassification, enhances hydrological consistency, and supports applications in flood risk assessment, soil erosion studies, and sustainable watershed management (Figure 5).

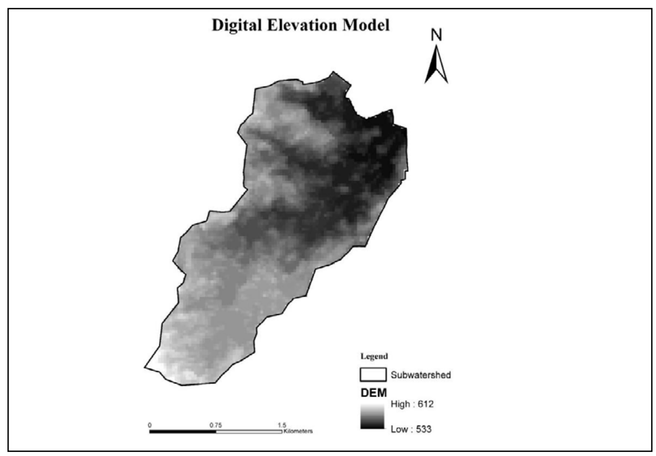

Figure 5: Digital elevation model of MPKV Central (West) watershed

3.2. Land use/land cover map

Land use/land cover and soil maps were used to determine curve numbers for runoff estimation using the NRCS method. Hydrologic soil groups A, B, C, and D were delineated within the Central MPKV watershed. A land use/land cover map, generated through GIS software, facilitated the computation of area distributions for each land use class. The details of land use/land cover categories and their area are presented in Table 4 and discussed as follows. In the present study, satellite imagery of Sentinel 2 MSI L1C was used to prepare the land use/land cover map. Merging of higher resolution data helped in better

Table 3: Spatial distribution of land use features in central MPKV watershed and corresponding CN values

LULC classes	HSG	CN	Area (km²)	% Area	% Weighted Area	WCN
Agricultural land	A	76	0.0383	0.8065	0.6129	AMC I=53.53
	B	86	0.0031	0.0651	0.0560	
	C	90	0.0180	0.3798	0.3419	AMC II=73.28
	D	93	0.0184	0.3880	0.3608	
Barren land	A	71	2.0072	42.2474	29.9957	AMC III=86.32
	B	80	0.2999	6.3120	5.0496	
	C	85	0.7729	16.2683	13.8280	
	D	88	0.1067	2.2455	1.9760	
Built up	A	69	0.3864	8.1337	5.6122	
	B	79	0.0368	0.7736	0.6112	
	C	84	0.1320	2.7779	2.3334	
	D	87	0.0265	0.5581	0.4855	
Forest	A	26	0.2512	5.2869	1.3746	
	B	40	0.0117	0.2453	0.0981	
	C	58	0.2658	5.5940	3.2445	
	D	61	0.0511	1.0757	0.6562	
Water bodies	A	97	0.1929	4.0611	3.9392	
	B	97	0.0142	0.2979	0.2889	
	C	97	0.0964	2.0297	1.9688	
	D	97	0.0216	0.4536	0.4400	
Total			4.7510	100.00		

Table 4: Distribution of land use patterns in the central MPKV watershed

Sl. No.	Land use/Land cover	Area (km²)	% Area
1.	Agriculture land	0.07789	1.64
2.	Barren land	3.18664	67.07
3.	Built up	0.58167	12.24
4.	Forest	0.57971	12.21
5.	Waterbodies	0.32507	6.84
	Total area	4.75098	100.00

classification of land use/land cover categories accurately. The study area was classified into 5 main categories, viz., agricultural land, barren land, forest, built-up, and waterbodies.

After the supervised classification of MSI L1C satellite image under ArcGIS software, the areal extent of land use types viz., Agricultural land, Barren land, built up area, Forest, and Waterbodies were found to be 0.07789, 3.18664, 0.58167, 0.57971, 0.32507 km^2 respectively (Table 4). The obtained results indicate that, watershed had more barren land area, followed by built-up area, and there was only a small portion of agricultural area. For classifying using a supervised method, the selected areas were identified by some ground truth values. The land use/land cover map of the study area using supervised classification is shown in Figure 6.

Similar methodologies have been used in other Indian watersheds; for example, in the REMI watershed, seven land use/cover classes were mapped and CN values computed for multiple Antecedent Moisture Conditions (Pandey and Sahu, 2009). In the Kanhaiya Nala watershed, unsupervised classification was used to map LULC, followed by CN estimation with soil group and land use data (Meshram et al., 2017). Also, Makandar and Kaman (2021) used Sentinel-2 and Landsat imagery, supervised classification (Maximum Likelihood), for similar classes and achieved ~ 88% overall accuracy in their LULC maps. These findings are consistent with recent research that highlights the effectiveness of Sentinel-2 imagery in LULC classification. Jocea et al. (2025) emphasized that Sentinel-2 data, when combined with supervised classification, provides operational reliability

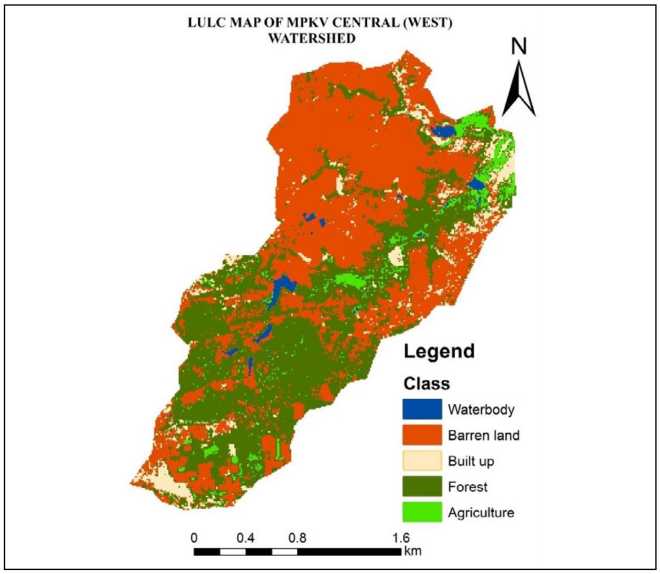

Figure 6: LULC map of MPKV Central (West) Watershed

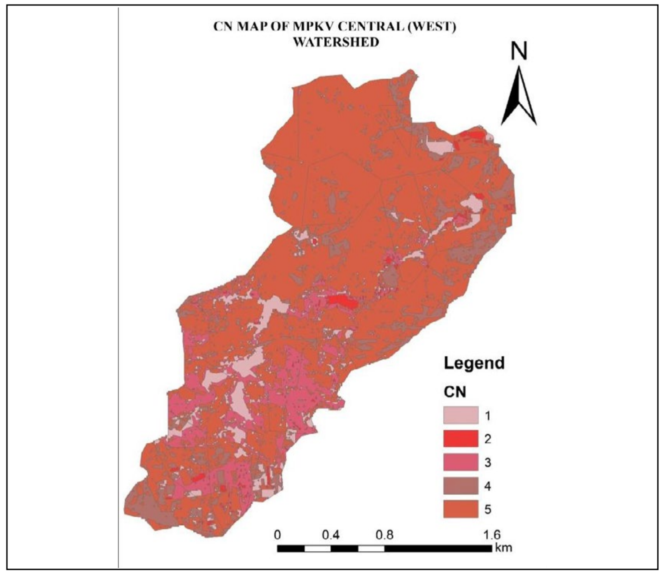

Figure 7: CN map of MPKV Central (West) Watershed

for watershed-scale studies. Additionally, Sawant and Ghosh (2024) demonstrated that deep learning approaches applied to Sentinel imagery enhance precision in urban and agricultural land mapping. Similarly, Gupta and Dixit (2022) generate LULC map which is classified into eight classes, validated by the value of overall accuracy and Kappa coefficient at 89.81% and 0.87, respectively.

3.3. CN values

Curve Numbers were assigned to the watershed as given in Table 3 for AMC condition II (I_a=0.2S), based on standard tables suggested by Soil Conservation Services, 1972.

The obtained CN map is shown in Figure 7. The weighted CN values are further corrected using the slope in m/m (initially estimated in degrees and then converted to radians).

Our findings are consistent with earlier work in India: for example, Mishra et al. (2014) demonstrated that slope-adjusted CN values in Roorkee plots yielded significantly more accurate runoff prediction, particularly in steeper plots. Memon et al. (2025) demonstrated that Sentinel-2 imagery improves classification accuracy in heterogeneous landscapes, particularly in Gujarat, where barren land dominated runoff potential. Similarly, recent GIS-based studies in central Iran showed that CN adjustment using slope functions improves agreement (e.g., higher NSE, lower RMSE) between predicted and observed runoff. These confirm that slope correction, combined with AMC, yields more realistic and sensitive runoff estimates than uncorrected CN methods (Forootan, 2023). The ESRI global 10m annual land cover dataset (2017–2024) derived from Sentinel-2 imagery shows widespread urban expansion and barren land dominance in semi-arid regions worldwide, increasing CN values and runoff potential. Jocea et al. (2025) reviewed Sentinel-2 applications globally, confirming that supervised classification remains a reliable approach for watershed-scale hydrological modeling.

3.4. Hydrologic soil group

It was observed that the watershed consists of Hydrologic Soil Group A, Soil Group B, Soil Group C, and Soil Group D, as shown in Figure 8.

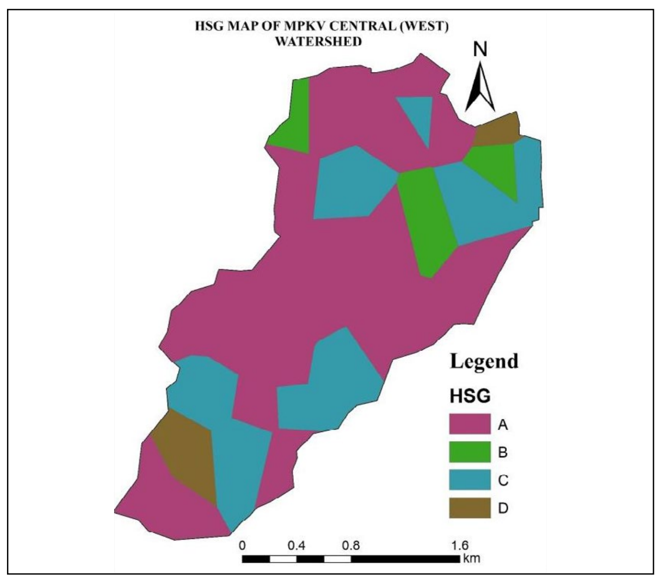

Figure 8: HSG map of MPKV Central (West) watershed

This method of delineating HSGs based on soil texture and integrating them with GIS is widely used in hydrological modeling. For example, Kumar et al. (2021) generated an HSG map for the Sind River Basin using NBSS and LUP soil data and classified soils into Groups A through D to support curve number-based runoff estimation. Similarly, Pandi et al. (2017) mapped HSGs in the Pennar Basin, Andhra Pradesh, to identify suitable runoff harvesting zones, using digitized soil data from the Watershed Atlas of India. Jocea et al. (2025) reviewed Sentinel-2 applications globally, confirming that supervised classification integrated with soil data remains reliable for watershed-scale hydrological modeling. Ross et al. (2018) developed the HYSOGs250m dataset, a globally consistent gridded map of hydrologic soil groups designed to support USDA CN-based runoff modeling. This dataset, with a resolution of 250 m, provides a robust framework for regional and continental hydrological studies.

3.5. *Runoff depth*

The Rainfall data for the year 2021 was collected from the IMD observatory located at AICRP on Irrigation Water Management, MPKV, Rahuri, and runoff was estimated by the SCS method. The annual rainfall for the year 2021 in the MPKV watershed was 966.40 mm, whereas the annual runoff was 278.97 mm, amounting to 28.86% of the total rainfall received. This value aligns with similar studies conducted across India.

3.5.1. *Total runoff estimation*

This study employed a modified SCS-CN (NRCS) model for rainfall-runoff estimation, integrating factors such as soil type, vegetation cover, slope, and watershed characteristics. The rainfall-runoff relationship was examined by accounting for initial abstraction, runoff, and actual retention. The curve number (CN) for the basin was derived through a combination of land use, soil type, and antecedent moisture conditions (AMC).

The study area consists of different land use/ land cover. About 67.07% area is occupied by Barren land, 12.24% by Built up, 12.21% by Forest, 6.84% by Waterbodies and the remaining 1.64% of the area is occupied by Agricultural Land. Hence, among the different land cover types, the Barren land plays the major role in the direct surface runoff. The SCS-CN method is used, and both Curve Number and weighted Curve Number are calculated based on the overlaid LULC map (Table 3). Weighted CN_I and weighted CN_{III} were calculated using the formula. Antecedent Moisture Condition (AMC) values were assigned according to the total rainfall received over the five days preceding the event. Weighted curve number values (CN_I, CN_{II}, and CN_{III}) with respect to the Antecedent Moisture Condition (AMC-I, AMC-II, and AMC-III) were found to be 53.53, 73.28, and 86.32, respectively. The annual rainfall for the year 2021 in the MPKV watershed was 966.40 mm, whereas the annual runoff was 278.97 mm, amounting to 28.86% of the total rainfall received, and the rainfall data is shown in Table 5.

Table 5: Monthly and annual rainfall and runoff (mm) for MPKV Central Campus (West) Watershed for the year 2023

Month	Rainfall, mm	Runoff, mm	Month	Rainfall, mm	Runoff, mm
Jan	20.6	3.75977	July	167.6	64.0965
Feb	7.2	0	Aug	157	58.9921
March	23.4	5.15095	Sept	245.4	78.5282
April	0	0	Oct	88.6	22.836
May	6.4	0	Nov	50.4	6.5532
June	129.2	17.0243	Dec	70.6	22.0274
Annual	Rainfall, mm	966.4	Runoff, mm	278.968	

The land use and land cover characteristics of the study area and its subdivisions are analyzed using the land use/ land cover (LU/LC) map presented in Figure 6, along with the associated statistical data. The LU/LC in the study area using the Sentinel 2 MSI L1C image shown in Figure 9 was classified into five classes, and the statistics were given in Table 4 and depicted in Figure 9. The agricultural land was in light green color, waterbodies with dark blue, forest with dark green, built up in dark red, and barren land in orange. The rainfall-runoff relationship was depicted in Figure 10.

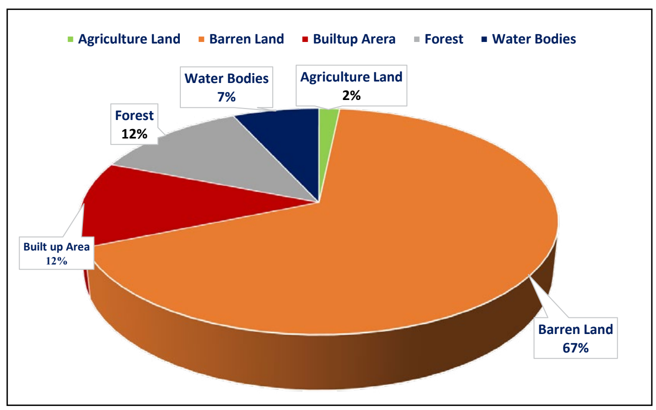

Figure 9: Pie chart of percent area in land use / land cover

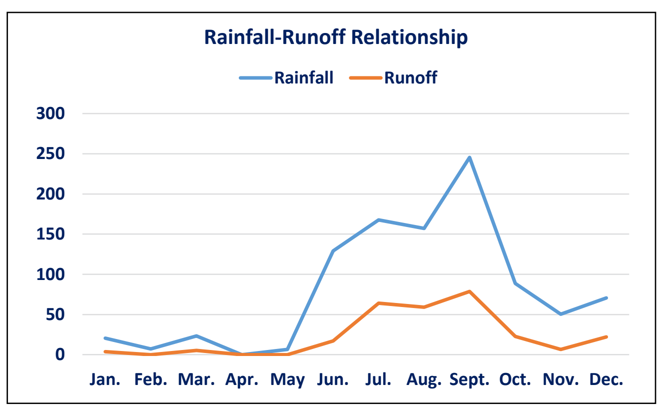

Figure 10: Rainfall-runoff relationship

In the MPKV Central Campus (West) watershed, the observed annual runoff (~279 mm) corresponds to about 29% of the annual rainfall (966 mm) becoming runoff. In comparison, in a semi-arid agricultural watershed in Northern India, 421.9 mm of runoff was reported out of ~1066.8 mm rainfall, i.e., about 39% runoff coefficient. Govindaraju et al. (2024) reported that runoff contributed about 30% of rainfall in the Kurumballi sub-watershed of Karnataka, while Indwar et al. (2022) found runoff ratios between 27–32% in the Tawa catchment of Madhya Pradesh. Similarly, Yadav and Dey (2025) estimated runoff at nearly 29% of rainfall in the Shilabati River Basin, West Bengal, using RS and GIS-based SCS-CN modeling. These studies highlight that semi-arid watersheds with significant barren and built-up land cover typically generate runoff in the range of 25–35% of annual rainfall. For instance, Kumar et al. (2021) estimated runoff in the Sind River Basin and reported a lower runoff coefficient of 17.21%, attributed to higher infiltration due to soil and land use conditions. Conversely, Pandi et al. (2017), studying the Pennar Basin in Andhra Pradesh, identified runoff potential ranging between 20–30%, which is comparable to the MPKV watershed.

(Mishra et al., 2017). In the Mandavi Basin, Andhra Pradesh, the average annual rainfall ranged from ~340 to 1008 mm and runoff from ~229 to 706 mm, yielding runoff coefficients often in the 20–70% range depending on land use and soil (Siddi Raju et al., 2018). Meanwhile, in the Vishwamitri River watershed of Gujarat, with average annual rainfall up to about 2170 mm, the runoff was between ~49 to ~800 mm for different years, implying much lower to moderate runoff coefficients, especially when rainfall was high and loss (infiltration, evapotranspiration) was large (Vishvam et al., 2015). Thus, your result (~29%) is within the lower to moderate range found in Indian watersheds: not unusually low, but indicating significant losses due to infiltration, evapotranspiration, or storage.

4. CONCLUSION

The annual runoff in the MPKV Central Campus (West) watershed for the year 2021 was 278.97 mm, amounting to 28.86% of the annual rainfall received, 966.40mm. Weighted curve number values CN_I, CN_{II}, and CN_{III} with respect to the AMC-I, AMC-II, and AMC-III were found to be 53.53, 73.28, and 86.32, respectively. This result suggested that runoff was directly proportional to the amount of rainfall received.

5. REFERENCE

Al-Ghobari, H., Dewidar, A., Alataway, A., 2020. Estimation of surface water runoff for a semi-arid area using RS and GIS-based SCS-CN method. Water 12(7), 1924. https://doi.org/10.3390/w12071924.

Bansode, A., Patil, K., 2014. Estimation of runoff by using SCS curve number method and arc GIS. International Journal of Scientific & Engineering Research 5(7), 1283–1287. https://www.researchgate.net/publication/290947015.

Chavda, D.B., Makwana, J.J., Parmar, H.V., Kunapara, A.N., Prajapati, G.V., 2016. Estimation of runoff for ozat catchment using RS and GIS-based SCS-CN method. Current World Environment 11(1). DOI: http://dx.doi.org/10.12944/CWE.11.1.26.

Chimdessa, C., Dibaba, Z., Dula, G., 2023. GIS-based identification of water harvesting potential area in the Bale lowland of south eastern Ethiopia. Geology, Ecology, and Landscapes 9(2), 476–492. https://doi.org/10.1080/24749508.2023.2209978.

Chow, V.T., Maidment, D.R., Mays, L.W., 1988. Applied hydrology, New York: McGraw-Hill; ISBN: 0071001743, 9780071001748. Available from https://books.google.co.in/books?id=cmFuQgAACAAJ.

Deshmukh, D.S., Chaube, U.C., Hailu, A.E., Gudeta, D.A., Kassa, M.T., 2013. Estimation and comparison of curve numbers based on dynamic land use land cover change, observed rainfall-runoff data, and land slope, Journal of Hydrology 492, 89–101. ISSN 0022-1694, https://doi.org/10.1016/j.jhydrol.2013.04.001.

Pandi, P., Saravanan, K., Mohan, K., 2017. Identifying runoff harvesting sites over the Pennar Basin, Andhra Pradesh, using the SCS-CN method. International Journal of Civil Engineering and Technology (IJCIET) 8(8), 65–73.

Fan, Y., Clark, M., Lawrence, D.M., Swenson, S., Band, L.E., Brantley, S.L., Brooks, P.D., Dietrich, W.E., Flores, A., Grant, G., Kirchner, J.W., Mackay, D.S., McDonnell, J.J., Milly, P.C.D., Sullivan, P.L., Tague, C., Ajami, H., Chaney, N., Hartmann, A., Hazenberg, P., McNamara, J., Pelletier, J., Perket, J., Rouholahnejad-Freund, E., Wagener, T., Zeng, X., Beighley, E., Buzan, J., Huang, M., Livneh, B., Mohanty, B.P., Nijssen, B., Safeeq, M., Shen, C., Verseveld, W.V., Volk, J., Yamazaki, D., 2019. Hillslope hydrology in global change research and earth system modeling. Water Resources Research 55(2), 1737–1772. DOI: https://doi.org/10.1029/2018WR023903.

Forootan, E., 2023. GIS-based slope-adjusted curve number methods for runoff estimation. Environmental Monitoring and Assessment 195(4), 489. doi: 10.1007/s10661-023-11039-6. PMID: 36939939.

Gabriels, K., Willems, P., Orshoven, J.V., 2021. Performance evaluation of spatially distributed, CN-based rainfall-runoff model configurations for implementation in spatial land use optimization analyses, Journal of Hydrology 602, 126872. ISSN 0022-1694, https://doi.org/10.1016/j.jhydrol.2021.126872.

Garg, V., Nikam, B., Thakur, P., Aggarwal, S., 2013. Assessment of the effect of slope on runoff potential of a watershed using the NRCS-CN Method. International Journal of Hydrology Science and Technology, SP-141, 3, 141–159. DO - 10.1504/IJHST.2013.057626.

Garzón, A., Kapelan, Z., Langeveld, J., Taormina, R., 2022. Machine learning-based surrogate modeling for Urban Water Networks: Review and future research directions. Water Resources Research 58, e2021WR031808. https://doi.org/10.1029/2021WR031808.

Govindaraju, Vinutha, T.Y., Rakesh, C.J., Lokanath, S., Kumar, A.K., 2024. Surface runoff estimation using SCS-CN method for kurumballi sub-watershed in Shivamogga District, Karnataka, India. Nature, Environment and Pollution Technology 23(2), 843–854. https://doi.org/10.46488/NEPT.2024.v23i02.020.

Grillakis, M.G., Koutroulis, A.G., Komma, J., Tsanis, I.K., Wagner, W., Bloschl, G., 2016. Initial soil moisture effects on flash flood generation-A comparison between basins of contrasting hydro-climatic conditions. Journal of Hydrology 541, Part A; 206–217. ISSN 0022-1694. https://doi.org/10.1016/j.jhydrol.2016.03.007.

Gupta, L., Dixit, J., 2022. Estimation of rainfall-induced surface runoff for the Assam region, India, using the GIS-based NRCS-CN method. Journal of Maps 18(2), 428–440. https://doi.org/10.1080/17445647.2022.2076624.

Gupta, M., Srivastava, P.K., Islam, T., 2015. Integrating remote sensing, GIS, and the SCS-CN method for runoff estimation in a semi-arid region of India. Environmental Earth Sciences 73(1), 2569–2581. https://doi.org/10.1007/s12665-014-3592-1.

Halder, S., Roy Chowdhury, A., Kar, S., Ray, D., Bhandari, G., 2024. Critical watershed prioritization through multi-criteria decision-making techniques and GIS integration for watershed management. Sustainability 16(8), Article 3467. https://doi.org/10.3390/su16083467.

Indwar, S.P., Kumar, A., Jaiswal, R., Galkate, R.V., Thomas, T., 2022. Rainfall–runoff modelling using SCS-CN and GIS approach in the Tawa catchment of Madhya Pradesh, India. Journal of Indian Water Resources Society 42(3–4), 45–56. https://iwrs.org.in/journal/juloct2022/5jul.pdf.

Jakir Hussain, K.N., Vijayakumari, R.C., Nagaraj, M., Varsha, S.R., Tejaswini, C., Jagadeesh, B.R., Basavaraj, D.B., 2024. Spatial analysis of surface runoff using SCS-CN technique integrated with GIS and remote sensing. International Journal of Environment and Climate Change 14(5), 441–454. https://doi.org/10.9734/ijecc/2024/v14i54204.

Jha, M.K., Chowdary, V.M., Kulkarni, Y., Mal, B.C., 2014. Rainwater harvesting planning using geospatial techniques and multicriteria decision analysis. Resources, Conservation and Recycling 83, 96–111. ISSN 0921-3449. https://doi.org/10.1016/j.resconrec.2013.12.003.

Jocea, A.F., Porumb, L., Necula, L., Raducanu, D., 2025. Sentinel-2 land cover classification: state-of-the-art methods and the reality of operational deployment-a systematic review. Sustainability 17(22), 10324. https://doi.org/10.3390/su172210324.

Kadam, A., Karnewar, A., Umrikar, B., Sankhua, R., 2019. Hydrological response-based watershed prioritization in the semiarid, basaltic region of western India using frequency ratio, fuzzy logic and AHP method. Environment Development and Sustainability, 21. 10.1007/s10668-018-0104-4.

Katpatal, Y.B., Paranjpe, S.V., Kadu, M., 2014. Validation of SCS CN method for runoff estimation with field observed regression analysis results in venna basin, central India. AGU Fall Meeting Abstracts. SP -H41E-0856. H41E-0856. https://ui.adsabs.harvard.edu/abs/2014AGUFM.H41E0856K.

Khalid, N., Abdul Halim, M., Shahimi, S.N.A., 2021. A comparative study of delineated watersheds using ASTER and SRTM in Johor, Malaysia. International Journal of Geospatial and Environmental Research, 8(2), Article 2. https://ijger-ojs-txstate.tdl.org/ijger/article/view/110.

Kumar, A., Kanga, S., Taloor, A.K., Singh, S.K., Đurin, B. 2021. Surface runoff estimation of Sind river basin using integrated SCS-CN and GIS techniques, HydroResearch 4, 61–74. ISSN 2589-7578, https://doi.org/10.1016/j.hydres.2021.08.001.

Makandar, A., Kaman, S., 2021. Land use land cover study of Sentinel-2a and Landsat-5 images using NDVI and supervised classification techniques. ICTACT Journal on Image and Video Processing 12(02), 2582–2587. DOI: 10.21917/ijivp 2021.0365.

Memon, A., Shah, N., Thakkar, D., Patel, Y., 2025. Statistical evaluation of open source DEMs for accurate watershed delineation in sustainable river basin management. Discover Geoscience 3(151). https://doi.org/10.1007/s44288-025-00276-6.

Memon, A.V., Shah, N.V., Patel, Y.S., Parangi, T., 2025. Enhancing land use/land cover analysis with sentinel-2 bands: comparative evaluation of classification algorithms and dimensionality reduction for improved accuracy assessment. Nature Environment and Pollution Technology 24(2), B4264. https://doi.org/10.46488/NEPT.2025.v24i02.B4264.

Meshram, S.G., Sharma, S.K., 2017. Prioritization of the watershed through morphometric parameters: A PCA-based approach. Applied Water Science 7(3), 1505–1519. https://doi.org/10.1007/s13201-015-0332-9.

Meshram, S.G., Sharma, S.K., Tignath, S., 2017. Application of remote sensing and geographical information systems for the generation of the runoff curve number. Applied Water Science 7, 1773–1779. https://doi.org/10.1007/s13201-015-0350-7.

Mishra, H., Denis, D.M., Suryavanshi, S., Kumar, M., Srivastava, S.K., Denis, A.F., Kumar, R., 2017. Hydrological simulation of a small ungauged agricultural watershed, Semrakalwana of Northern India. Applied Water Science 7(6), 2803–2815. https://doi.org/10.1007/s13201-017-0531-7.

Mishra, S.K., Chaudhary, A., Shrestha, R.K., Pandey, A., Lal, M., 2014. Experimental verification of the effect of slope and land use on SCS runoff curve number. Water Resources Management 28, 3407–3416. https://doi.org/10.1007/s11269-014-0582-6.

Mishra, S.K., Singh, V.P., 2003. Soil conservation service curve number (SCS-CN) methodology. Water Science and Technology Library, Vol. 42. Springer. http://dx.doi.org/10.1007/978-94-017-0147-1.

Muneer, A.S., Sayl, K.N., Kamel, A.H., 2020. Modeling of runoff in the arid regions using remote sensing and geographic information systems (GIS). International Journal of Design & Nature and Ecodynamics 15(5), 691–700. https://doi.org/10.18280/ijdne.150511.

Nasrin, M., Barman, B., 2023. Digital terrain analysis to understand watershed characterization using ASTER DEM: A case study of Jamuna watershed of Assam, India. International Journal of Innovative Research in Technology 11(9), 1365–1370. https://ijirt.org/article?manuscript=172915.

Nikita, D.P., Ayare, B.L., Bhange, H.N., Ingle, P.M., Tharkar, M.H., Gavit, S.B., 2024. Runoff estimation in kajurli watershed using SCS-CN and GIS techniques. International Journal of Environment and Climate Change 14(10), 547–556. https://doi.org/10.9734/ijecc/2024/v14i104507.

Pandey, A., Sahu, A.K., 2009. Generation of curve number using Remote Sensing and Geographic Information System. Geospatial World. https://geospatialworld.net/article/ generation-of-curve-number- using-remote-sensing-and-geographic-information-system/?utm_source=chatgpt.com.

Pandey, B.K., Dabral, P.P., Pandey, D.C., 2021. Integrated approach to simulate hydrological responses: Surface runoff and evapotranspiration. Journal of Hydrology 598, 126380. https://doi.org/10.1016/j.jhydrol.2021.126380.

Raushan, R., Rohit, K., Aishwarya, M., Manda A., Srivalli, C., 2024. An artificial neural network and SCS–CN-based model for runoff estimation: a case study of the Peddavagu watershed. Water Practice and Technology 19(7), 2734–2743. doi: https://doi.org/10.2166/wpt.2024.167.

Reddy, K.H.N., Kothari, M., Reddy, K.S., Singh, P.K., Yadav, K.K., 2020. Assessment of Surface runoff using ArcSWAT for rela watershed, Rajasthan, India. Journal of Geography, Environment and Earth Science International 24(10), 22–32. https://doi.org/10.9734/jgeesi/2020/v24i1030260.

Ross, C.W., Prihodko, L., Anchang, J.Y., Kumar, S.S., Ji, W., Hanan, N.P., 2018. Global hydrologic soil groups (HYSOGs250m) for curve number-based runoff modeling (Version 1). ORNL Distributed Active Archive Center. https://doi.org/10.3334/ORNLDAAC/1566.

Satheeshkumar, S., Venkateswaran, S., Kannan, R., 2017. Rainfall-runoff estimation using SCS-CN and GIS approach in the Pappiredipatti watershed of the Vaniyar sub-basin, South India. Model Earth Systems and Environment 3, 24. https://doi.org/10.1007/s40808-017-0301-4.

Sawant, S., Ghosh, J.K., 2024. Land use land cover classification using Sentinel imagery based on deep learning models. Journal of Earth System Science 133, 101. https://doi.org/10.1007/s12040-024-02298-z.

Siddi Raju, R., Sudarsana, Raju, G., Rajasekhar, M., 2018. Estimation of rainfall runoff using SCS CN method with RS and GIS techniques for mandavi basin in YSR Kadapa District of Andhra Pradesh, India. Hydrospatial Analysis 2(1), 1–15. https://doi.org/10.21523/gcj3.18020101.

Shaikh, A.A., Pathan, A.I., Waikhom, S.I., Rathod, P., 2022. Comparison of watershed delineation and drainage network using ASTER and CARTOSAT DEM of Surat City, Gujarat. In: Vasant, P., Zelinka, I., Weber, GW. (Eds), Intelligent computing & optimization. ICO 2021. Lecture Notes in Networks and Systems 371, 788–800. Springer, Cham. https://doi.org/10.1007/978-3-030-93247-3_75.

Shiv, S.B., Mahesh, T., Rishi, P., 2023. Estimation of runoff using USDA SCS-curve number and autoregressive time series model parameters for Kachhinda watershed, Morena District, Madhya Pradesh, India. International Journal of Environment

and Climate Change 13(10), 2939–2948. https://doi.org/10.9734/ijecc/2023/v13i102960.
Singh, A., Tiwari, K.N., Mal, B.C., 2023. Modification of the SCS-CN method using soil moisture accounting and rainfall intensity variation for improved runoff simulation. Water 15(13), 2374. https://doi.org/10.3390/w15132374.
Singh, H., Alam, M.A., Sharma, P.J., Rautela, K.S., 2023. A comparison of the SCS-CN-based models for hydrological simulation of the Aghanashini River, Karnataka, India. AQUA-Water Infrastructure, Ecosystems and Society 72(4), 507–519. doi: https://doi.org/10.2166/aqua.2023.213.
Sishah, S., 2021. Rainfall runoff estimation using GIS and SCS-CN method for awash river basin, Ethiopia. International Journal of Hydrology 5(1), 33–37. DOI: 10.15406/ijh.2021.05.00263.
Srivastava, R.K., Imtiyaz, M., 2016. Testing of the coupled SCS Curve Number model for estimating runoff and sediment yield for eleven watersheds. Journal of the Geological Society of India 88(5), 627–636. https://doi.org/10.1007/s12594-016-0529-z.
Soulis, K.X., 2021. Soil conservation service curve number (SCS-CN) Method: Current applications, remaining challenges, and future perspectives. Water 13(2), 192. https://doi.org/10.3390/w13020192.
Soulis, K.X., Valiantzas, J.D., Dercas, N., Londra, P.A., 2009. Investigation of the direct runoff generation mechanism for the analysis of the SCS-CN method applicability to a partial area experimental watershed. Hydrology and Earth System Sciences 13(5), 605–615. https://doi.org/10.5194/hess-13-605-2009.
Sun, T., Deng, L., Fei, K., Fan, X., Zhang, L., Ni, L., Sun, R., 2021. Runoff characteristics and soil loss mechanism in the weathered granite area under simulated rainfall. Water 13(23), 3453. https://doi.org/10.3390/w13233453.
Vishvam, H.P., Pradeep, P.L., Indra, P., 2015. Estimation of runoff and soil erosion for vishwamitri river watershed, western India using RS and GIS. American Journal of Water Science and Engineering 1(2), 7–14. https://doi.org/10.11648/j.ajwse.20150102.11.
Wang, Q., Zhao, X., Li, F., Zhao, W., Awuku, I., Ma, W., Liu, Q., Liu, B., Cai, T., Liu, Y., Li, X., 2025. Optimized parameters for SCS-CN model in runoff prediction in ridge-furrow rainwater harvesting in semiarid regions of China, Agricultural Water Management 310, 109363. ISSN 0378-3774, https://doi.org/10.1016/j.agwat.2025.109363.
Yadav, V., Dey, S., 2025. Estimating rainfall, surface runoff, and river discharge in the Shilabati river basin using an integrated RS and GIS-based SCS-CN approach. Discover Geoscience 3, Article 177. https://doi.org/10.1007/s44288-025-00291-7.